ACTA ABP BIOCHIMICA POLONICA

Vol. 60, No 4/2013
701–706
on-line at: www.actabp.pl

Regular paper

Differences in metabolic profiles of planktonic and biofilm cells in *Staphylococcus aureus* — ^{1}H Nuclear Magnetic Resonance search for candidate biomarkers*

Adam Feliks Junka[1]✉, Stanisław Deja[2], Danuta Smutnicka[1], Patrycja Szymczyk[3], Grzegorz Ziółkowski[3], Marzenna Bartoszewicz[1] and Piotr Młynarz[2]

[1]Department of Microbiology, Medical University of Wroclaw, Wrocław, Poland; [2]Faculty of Chemistry, Opole University, Opole, Poland; [3]Wroclaw University of Technology, Centre for Advanced Manufacturing Technologies, Wrocław, Poland; [4]Department of Bioorganic Chemistry, Faculty of Chemistry, Wroclaw University of Technology, Wrocław, Poland

***Staphylococcus aureus* is responsible for many types of infections related to biofilm presence. As the early diagnostics remains the best option for prevention of biofilm infections, the aim of the work presented was to search for differences in metabolite patterns of *S. aureus* ATCC6538 biofilm *vs.* free-swimming *S. aureus* planktonic forms. For this purpose, Nuclear Magnetic Resonance (NMR) spectroscopy was applied. Data obtained were supported by means of Scanning Electron Microscopy, quantitative cultures and X-ray computed microtomography. Metabolic trends accompanying *S. aureus* biofilm formation were found using Principal Component Analysis (PCA). Levels of isoleucine, alanine and 2,3-butanediol were significantly higher in biofilm than in planktonic forms, whereas level of osmoprotectant glycine-betaine was significantly higher in planktonic forms of *S. aureus*. Results obtained may find future application in clinical diagnostics of *S. aureus* biofilm-related infections.**

Key words: *Staphylococcus aureus*, biofilm, NMR, metabolomics, glycine-betaine

Received: 31 October, 2013; revised: 25 November, 2013; accepted: 12 December, 2013; available on-line: 30 December, 2013

INTRODUCTION

Biofilm is dynamic, surface-associated community of microorganisms embedded in layers of extracellular slime. Biofilms develop not only at solid-water interfaces (substrate-associated biofilms), but also, as the floating biofilms, at the water-air interface (Declerck *et al.,* 2010). Thanks to protective architecture, layer-dependent differences in metabolic activity and easiness of gene exchange, adhered bacteria display higher resistance against immune system and antimicrobials than their planktonic or so called "free-swimming" counterparts (Bjarnsholt *et al*., 2012). Therefore, the biofilm is responsible for particularly hard-to-treat infections, including these related to the presence of implants (Shunmuganperumal *et al*., 2010). Biofilm's ability to persist on various medical devices and to evade antimicrobials, provides satisfactory explanation for a high number of therapeutic failures, which could not be explained otherwise. Although many counteractive measures are developed, including false metabolites, anti-Quorum Sensing agents, detergents and enzymes, biofilm remains one of the greatest challenges of contemporary medicine (Wolcott *et al*., 2010). The early diagnostics remains still the best protection from biofilm-related infections. Active therapies should be applied before biofilm matures; but when it happens, sharp surgical debridement or medical implant removal are often the only options left (Widegrow *et al*., 2008; Wolcott *et al*., 2010).

Among many opportunistic pathogens, Gram-positive *Staphylococcus aureus* is considered to be one of the leading factors of orthopedic, wound and catheter-related infections. All these infections are, in fact, related to the biofilm presence (Montaro *et al*., 2011). Increasing percentage of *S. aureus* strains displays also specific antibiotic resistance against β-lactamase antibiotics. Such strains are referred to as Methicilin Resistant *Staphylococcus aureus* (MRSA). Thus, once matured, MRSA biofilm is particularly hard to eradicate (Mahmoud *et al*., 2012).

Hence, it is of paramount importance to enrich body of knowledge concerning *S. aureus* pathogenicity. Analysis of differences between *S. aureus* plankton and biofilm is one of the directions to follow, as it may be applied in future schemes of diagnostics and treatment. A lot of work has been performed on the subject so far (Resch *et al*., 2005; Secor *et al*., 2011; Sadowska *et al*., 2013), however, there is still plenty of work to be done. Particularly, metabolomics of *S. aureus* planktonic forms and biofilm remains one of the fields for further studies.

Metabolome is a set of both intra- and extracellular metabolites of a living system (Nicholson *et al*., 1999; Fiehn *et al*., 2002). Part of a system biology referred to as metabolomics is focused on comprehensive analysis of these low molecular weight metabolites (MW<1500 Da). Usefulness of metabolomics approach has been demonstrated in the field of disease diagnostics (Bertini *et al*., 2012), determination of food origin (Schievano *et al*., 2012), quality control (Li *et al*., 2013), and many others. Nuclear Magnetic Resonance (NMR) spectroscopy is one of the fundamental tools among all analytical methods used in metabolomics studies.

NMR technique uses radiofrequency waves to acquire information about magnetic nuclei. It allows to observe not only a specific nuclei, but also their distribution across all chemical compounds present in the analyzed sample. Moreover, signals are sensitive to local chemical

✉e-mail: feliks.junka@gmail.com

*Presented at the 3-rd Workshop on Microbiology „MIKROBIOT 2013" in Łódź, Poland.

Abbreviations: MRSA, Methicilin Resistant *Staphylococcus aureus*; NMR, Nuclear Magnetic Resonance; *S. aureus, Staphylococcus aureus*

environment. NMR-based observation of these phenomena provides useful information concerning chemical structure of the compound. Therefore, data provided by NMR finds wide application in biological studies (Griffin, 2010).

By means of NMR spectroscopy, bacterial fingerprints and footprints may be also analyzed. Term "fingerprint" describes the metabolites inside the bacterial cells, whereas "footprint" refers to the metabolites secreted to the environment.

As for the biofilm study, recent review made by Zhang underlines the potency of a NMR spectroscopy in enhancing the understanding of a processes related to the structure and formation of the biofilms (Zhang, 2012). Therefore, the aim of presented study was to compare metabolic profiles of *S. aureus* biofilm and its planktonic forms, and to identify differences distinguishing one state of bacterial organization from another.

MATERIALS AND METHODS

Biofilm formation and quantitative cultures. Reference *S. aureus* ATCC 6538 strain, cultured on the stable CA medium (Biocorp, Poland), was transferred to the liquid Enrichment Broth (Biocorp, Poland) and incubated at 37°C for 24 hours under the aerobic conditions. Density of bacterial suspension was measured using a densitometer (Biomerieux, Poland), and diluted to 3×10^8 cells/mL. Polystyrene mesh made of monofilamentous polipropylene of 0.46 mm macropores (Polernia, Poland) was used as a scaffold for the biofilm formation. Mesh was transferred to the bacterial suspension and left for 1, 2, 4, 8, 16 and 24 hours/37°C. After incubation, mesh was rinsed thoroughly, using physiological saline to remove the non-adhered bacteria. Subsequently, mesh was transferred to 1 mL of mild detergent (0.5% saponine, Sigma-Aldritch) and vortex mixed vigorously for 1 min. to detach biofilm. After vortex mixing, bacterial suspensions obtained were diluted 10 to 10^8 times. 100 μL of each dilution was cultured on the agar plate and incubated for 24 hours/37°C. After this time, bacterial colonies were counted, and the number of bacterial cells forming biofilm on the mesh was determined. All measurements were repeated 3 times and presented in the form of mean value of cfu (colony forming units).

X-ray computed microtomography (μCT). The aim of this assessment was to estimate the exact surface of used polystyrene mesh. Such approach allows to present data obtained by means of quantitative culturing as cfu/mm^2. This value provides more information concerning distribution of biofilm cells than value of cfu itself. To estimate surface of mesh, computed micro-tomography methods (μCT) were used. 3 samples of meshes were scanned using μCT system (Metrotom 1500, Carl Zeiss, Oberkochen, Germany). This system consists of a flat panel detector with a resolution of 1024×1024 px (400 μm pixel size) and 16bit grayscale, rotary table, and microfocus X-ray tube with maximal accelerating voltage 225 kV and maximal current 1000 μA. In order to achieve maximum resolution, the tube voltage was fixed on the level 220 kV and the current 120 μA. Number of projections performed during the rotation of the sample of 360° was 800 with 1 s integration time for each. The result matched the parameters permitted to achieve a voxel size of 31 microns. The obtained data were analyzed using software VG Studio MAX (Volume Graphics GmbH, Heidelberg, Germany).

Preparation of samples for footprint and fingerprint metabolic analysis. Staphylococcal biofilm was incubated on polystyrene mesh in conditions described in the part "quantitative cultures". Mesh with biofilm was rinsed on it with 0.9% NaCl to remove non-adherent bacteria. Next, mesh was transferred to 1 mL of H_2O and placed at –80°C untill the time of further analysis. Such samples are later referred to as "the biofilm" or "B".

In the liquid media, where meshes were introduced to, planktonic forms of *S. aureus* were also present. The cell-containing medium was centrifuged for 10 min/4440 g. Obtained cell-free supernatant was frozen at –80°C. Such samples are later referred to as "the medium" or "M". Centrifuged planktonic cells were rinsed with saline to remove medium traces, then centrifuged again and frozen at –80°C. These samples are later referred to as "the planktonic form" or "P".

Scanning Electron Microscopy. Staphylococcal biofilm was incubated on polystyrene mesh in conditions described in the part "quantitative cultures". Mesh with biofilm was rinsed on it with 0.9% NaCl to remove non-adherent bacteria. Subsequently, samples were allowed to dry at 37°C for 2 hours in sterile conditions. Dried samples were covered with Au/Pd (60:40, sputter current: 40 mA, sputter time: 50 sec) using QUORUM machine (Quorum International, USA), and examined on Scanning Electron Microscope Zeiss EVO MA25 (Carl Zeiss, Poland). The 25 neighbouring areas, and 25 randomly chosen areas of each sample were analyzed.

Preparation of NMR samples. Biofilm samples, collected after 1, 2, 4, 8, 16 and 24 hours of incubation, were transferred into a mechanic steel bead homogenizer (Tissuelyser LT; QIAGEN, Hilden, Germany). During the homogenization, samples were disrupted for 10 min. at 50 Hz shaking frequency. Samples were centrifuged at 25590 g/10 min. (Universal 32, Hettich, Germany). To 600 μL of supernatant obtained, 30 μL of phosphate buffer solution (PBS), and 70 μL of D_2O, containing trimethylsilyl-2,2,3,3-tetradeuteropropionic acid sodium salt (TSP, internal standard) were added. The planktonic samples were prepared in the analogical manner. After process of preparation, biofilm and planktonic samples were ready for fingerprint analysis. 600 μL of samples for footprint analysis (medium) were simply introduced to the eppendorf tube containing 30 μL of PBS buffer and 70 μL of D_2O.

^{1}H NMR measurements and data preprocessing. All NMR spectra were recorded at 300 K using Bruker Biospin Avance II NMR spectrometer (Bruker, GmBH, Germany) operating at proton frequency of 600.58 MHz. Biofilm and planktonic samples were measured using one-dimensional noesy pulse sequence with water presaturation, while medium samples were measured using Carr-Purcell-Meiboom-Gill (CPMG) pulse sequence in order to filter protein signals out. Number of scans was set at 128 and 64 for fingerprint and footprint, respectively. After Fourier transformation of spectra, baseline and phase were manually corrected using the Topspin 1.3 software (Bruker, GmBH, Germany). The whole spectral set was shifted to the TSP signal ($\delta = 0$ ppm). Next spectra were exported to Matlab (Matlab v.8.1, Mathwork Inc.), where residual HDO resonance was excluded (region 4.20–5.19 ppm). Data were normalized to constant sum of signals equal to 100.

Chemometrics and statistics. The STATISTICA software (v 10, StatSoft, Tulsa, USA) was utilized for the statistical analysis of the quantified metabolites (in terms of signal integrals). Metabolites were checked for

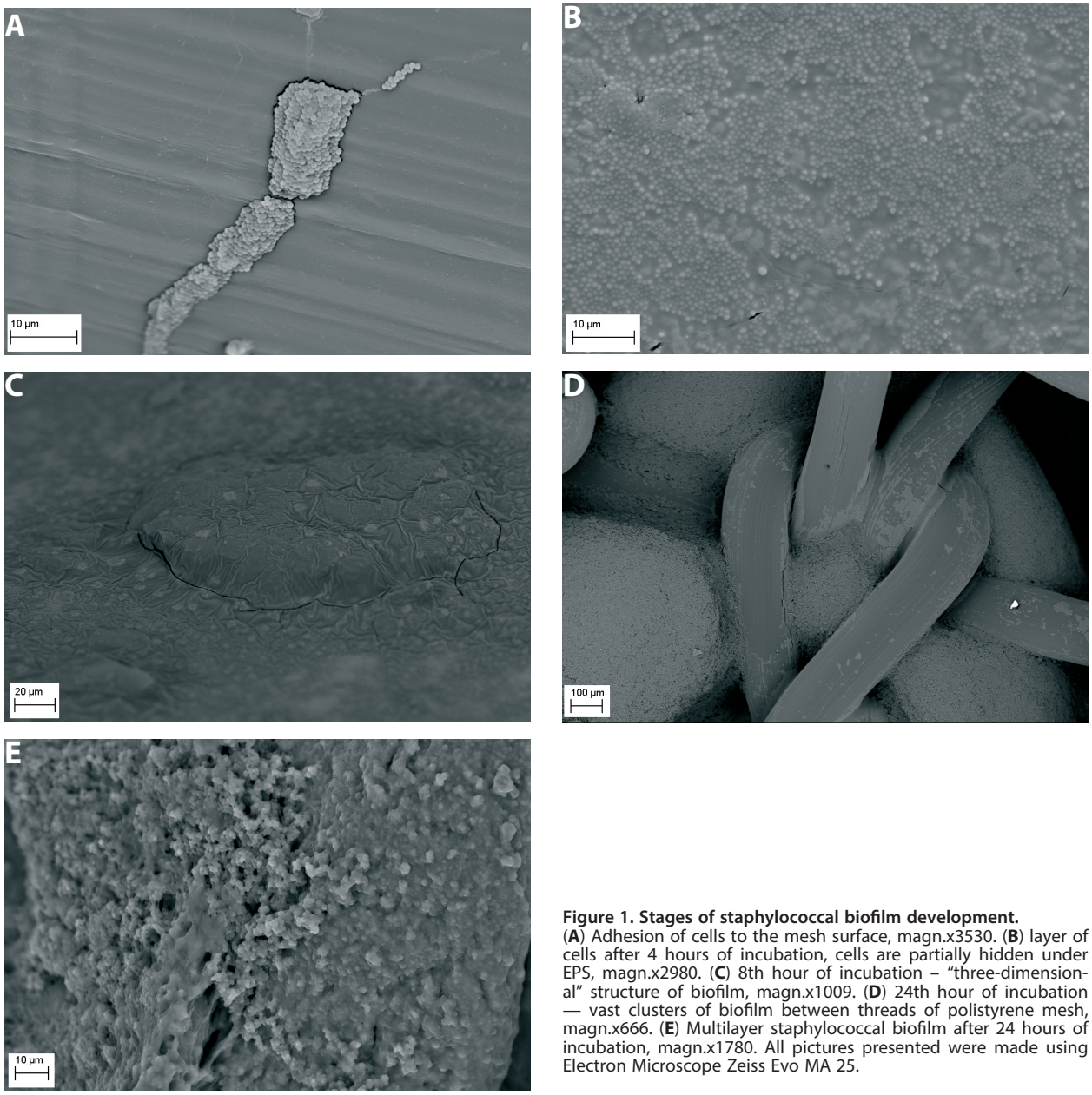

Figure 1. Stages of staphylococcal biofilm development.
(**A**) Adhesion of cells to the mesh surface, magn.x3530. (**B**) layer of cells after 4 hours of incubation, cells are partially hidden under EPS, magn.x2980. (**C**) 8th hour of incubation – "three-dimensional" structure of biofilm, magn.x1009. (**D**) 24th hour of incubation — vast clusters of biofilm between threads of polistyrene mesh, magn.x666. (**E**) Multilayer staphylococcal biofilm after 24 hours of incubation, magn.x1780. All pictures presented were made using Electron Microscope Zeiss Evo MA 25.

statistical significance using Mann−Whitney-Wilcoxon test (α=0.01). For multivariate data analysis Pareto scaling was used. Data were visualized using principal component analysis (PCA) in SIMCA-P+ software (v 13.0, Umetrics, Umeå, Sweden).

RESULTS

Biofilm dynamics

After one hour of incubation, staphylococcal cells adhered strongly to the surface of polystyrene mesh as it is shown in Fig. 1A. During the 2nd and the 4th hour of incubation, number of adhered staphylococcal cells increased approximately 10 times and 100 times, respectively. Surfaces coated with extracellular substance were seen among monolayers of adhered cocci, indicating process of biofilm maturation (Fig. 1B). Between 4th and 8th hour of incubation, number of cells grew rapidly reaching value of over 20 millions of cells/mm^2 of mesh surface. It means that staphylococcal cells have formed multilayer structure, typical for matured biofilm. Majority of cells were embedded within extracellular substance (Fig. 1C). Between 16th–24th hour of incubation, number of cells in biofilm has grown slightly. It suggests that biofilm has reached the plateu phase. Biofilm has formed vast clusters, seen even under relatively low mag-

Table 1. *Staphylococcal* biofilm dynamics expressed as number of colony units/mm^2 of polystyrene mesh.
Surface of mesh = 68.57 mm^2. S.D. — standard deviation

Incubation time (h)	Mean Cfu/mm^2	S.D.
1	3.6x10^3	385
2	29.1x10^3	1.4x10^3
4	8.7x10^5	81.1x10^3
8	20.9x10^6	4.4x10^6
16	52.5x10^6	6.6x10^6
24	64.1x10^6	5.8x10^6

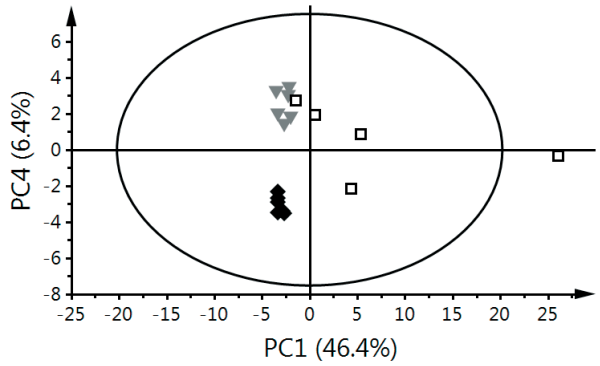

Figure 2. PCA score plot; white squares — planktonic fingerprint; gray triangles — biofilm fingerprint; black diamonds — footprint medium.
PC1 explains differences between planktonic fingerprint *vs*. all other types of samples analyzed. **PC4** allows to distinguish between fingerprints (both planktonic and biofilm) *vs*. footprint (medium). The samples displaying similar metabolomic profile are presented on the plot as proximal elements, whereas samples displaying significant differences are presented as distant elements.

nifications (Fig. 1D, E). Exact numbers of staphylococcal cells forming biofilm on the mesh surface are given in the Table 1.

NMR assessment

Protein content in footprint (medium) was higher than in fingerprint. Utilization of CPMG pulse sequence enabled to filter out signals originating from macromolecules and to compare footprint (medium) and fingerprint (biofilm and planktonic forms) spectra. The metabolites identified in the spectra are listed in Table 3. Observed differences between analyzed groups are visualized in PCA score plot (Fig. 2). First principal component (PC1) explains 46.4% of variance of this dataset. PC1 was mainly related to differences between planktonic fingerprint (P) *vs*. all other samples (B+M). It was impossible to distinguish biofilm fingerprint (B) from footprint (M) until the fourth principal component (PC4) was used. By explaining 6.4% of variance, PC4 made discrimination between samples B and P possible.

Planktonic fingerprint samples presented strongest dispersion in PCA score plot. This phenomenon was related to highest variability in terms of metabolite levels. Planktonic fingerprint spectra displayed low concentration of intracellular metabolites in the beginning and in the end of the experiment, and the higher concentration of metabolites between 4th and 8th hour were observed. Concentration of metabolites in samples collected in this time interval was similar to concentration of metabolites in biofilm fingerprint. Contrary to planktonic cells, biofilm cells exhibited stable concentration level of intracellular metabolites during whole experiment. Moreover, the biofilm fingerprint (B) was much more similar to footprint (M) than planktonic fingerprint (P).

Ten out of 15 metabolites examined, were affected significantly, at least in one of statistical tests performed (Table 2). Generally, there was a higher concentration of isoleucine, methionine, alanine, glucose, tyrosine and phenylalanine found in medium in comparison to either biofilm or plankton samples. Biofilm fingerprint displayed elevated level of isoleucine, 2–3 butanediol and alanine. Glycine-betaine was the only metabolite, which level was higher in planktonic forms than in biofilm.

DISCUSSION

It is estimated that 99.9% of bacterial biomass is organized in the biofilm form and at least 80% of all nosocomial infections are, in fact, biofilm-related infections (Bjarnsholt, 2011). This discovery has already changed face of contemporary microbiology, and it is presently changing current clinical approach to chronic infection treatment. Therefore, it is of great importance to increase our knowledge concerning process of biofilm formation. Every data related to this topic may find application in

Table 2. Staphylococcal metabolites identified.
B — biofilm; P — planktonic form; M — medium. B *vs*. P — comparison of metabolite level in biofilm fingerprint *vs*. planktonic fingerprint; B *vs*. M — comparison between biofilm fingerprint and. medium footprint; P *vs*. M — comparison between planktonic fingerprint and medium footprint. ↑ — higher level of metabolite in the specific sample; s — singlet; d — doublet; t — triplet; m — multiplet; q — quartet; dd — double doublet; *difference in metabolite level is statistically significant; n/s — non significant difference in metabolite level between specific samples. *P* value < 0.01, Mann-Whitney-Wilcoxon test.

No	Metabolite	Chemical shift (multiplicity)	B vs. P	B vs. M	P vs. M
1	Valine	0.99 (d), 1.04 (d)	n/s	n/s	n/s
2	Isoleucine	0.94 (t), 1.01 (d)	B↑ *	M↑ *	M↑ *
3	2,3-butanediol	1.14 (d)	B↑ *	n/s	M↑ *
4	Ethanol	1.19 (t), 3.66 (q)	n/s	n/s	n/s
5	Lactate	1.33 (d), 4.12 (q)	n/s	n/s	M↑ *
6	Methionine	2.14 (s)	n/s	M↑ *	M↑ *
7	Alanine	1.48 (d)	B↑ *	M↑ *	M↑ *
8	Acetate	1.9 (s)	n/s	n/s	n/s
9	Acetone	2.23 (s)	n/s	n/s	n/s
10	Glycine betaine	3.27 (s), 3.90 (s)	P↑ *	n/s	P↑ *
11	Glucose	3.25 (dd), 3.50 (t), 5.24 (d)	n/s	M↑ *	M↑ *
12	Tyrosine	6.90 (d), 7.20 (d)	n/s	M↑ *	M↑ *
13	Phenylalanine	7.33 (m), 7.38 (m), 7.43 (m)	n/s	M↑ *	M↑ *
14	Glycine	3.57 (s)	n/s	n/s	n/s
15	Succinate	2.41 (s)	n/s	M↑ *	n/s

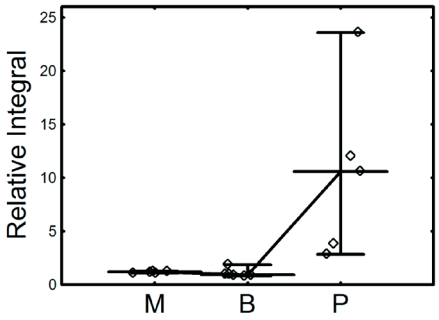

Figure 3. Differences in level of glycine-betaine in biofilm, medium and plankton samples.
Bar — median; whiskers — min max. **M** — medium, **B** — biofilm, **P** — planktonic forms. Note that even the lowest value of glycine-betaine in **P** samples is still higher than in **M** or **B** samples.

currently developed, biofilm-oriented diagnostics and treatment procedures (Wolcott, 2008; Bjarnsholt, 2010).

S. aureus strain used in the presented work was able to form biofilm on the surface of polystyrene mesh. Moreover, by means of electron microscopy and quantitative cultures, observation of the particular stages of biofilm formation was possible. Use of ^{1}H NMR spectroscopy allowed to discriminate between biofilm forms of *S. aureus* and its planktonic counterparts (Fig. 2). Such knowledge has got an applicative potential. The current reports indicate possibility of rapid identification of bacteria using ^{1}H NMR spectroscopy (Gupta *et al.*, 2012). In turn, our findings, if developed, would allow to distinguish whether *S. aureus* is undergoing process of biofilm formation or if it has formed mature biofilm already. Such knowledge given to the clinician, would allow him to change the antimicrobial treatment, e.g. to switch from biofilm-inefficient antibiotic therapy to techniques more appropriate for biofilm eradication, such as surgical debridement and antisepsis (Jawien *et al.*, 2012).

The results presented in Tab.2 are of more basic science character. As it was mentioned before, fingerprint metabolites are intracellular metabolites of planktonic forms or biofilm of *S. aureus*. But it should be borne in mind that in *in vitro* setting used, footprint metabolites comprise of metabolites secreted outside by planktonic cells, biofilm cells and metabolites present in, intact medium. However, analysis of metabolite levels (Table 2) may provide interesting information.

Level of succinate was found to be lower in biofilm than in planktonic forms and media. This result stays in line with data provided by Gaupp *et al.*, 2010. As it was shown in their study, succinate dehydrogenase activity was significantly up-regulated in *S. aureus* biofilm.

Levels of typical fermentation products, such as ethanol or acetate, was similar for biofilm and planktonic forms. Oxygen penetration to basal layers of biofilm is very limited, so presence of above mentioned metabolites seems to be natural phenomenon. In turn, presence of these metabolites in planktonic fingerprint may be explained by a growing number of cells in medium and subsequent decreasing concentration of oxygen. The 2,3-butanediol, another metabolite related to anaerobic fermentation of glucose, was found to be elevated in biofilm comparing to planktonic forms, and it may be so because of reasons explained above. Glucose itself was found in similar concentration in either biofilm and planktonic mode of growth. The highest concentration of this carbohydrate was found in medium. It seems to be justified, as liquid enrichment broth applied contained high 1% (w/v) of glucose content. The observed high level of lactate in medium may be also related with glucose consumption both by planktonic forms and biofilm (Gaupp *et al.*, 2010).

Two metabolites, other than 2,3-butanediol, were found in higher concentration in biofilm than in planktonic forms. These were alanine and isoleucine. Gross *et al.*, 2001, has proved that *S. aureus* mutant lacking D-alanine esters of teichoic acids is no longer able to adhere and form biofilm on abiotic surfaces. Therefore, presence of high level of alanine in biofilm seems to have rational explanation.

In turn, Pohl *et al.* (2009) showed that isoleucine plays a role in *Staphylococcus aureus* CodY-dependent repression of nitrogen metabolism. It is known that nitrite, either as the endogenous product of respiratory nitrate reduction or after external addition, is one of the factors impairing process of *S. aureus* biofilm formation (Schlag *et al.*, 2007). As it was shown in the presented work (Fig. 1, Table 1), *S. aureus* strain formed strong structures of biofilm on the abiotic mesh. Thus, our finding may indicate a role of isoleucine as biofilm dispersal down-regulator.

The phenylalanine and the tyrosine are two known inhibitors of *S. aureus* biofilm formation (Hochbaum *et al.,* 2011). These metabolites were found in the lower level in biofilm samples in comparison to medium. However, level of these two compounds were also lower in plankton than in medium.

The only metabolite found to be elevated in planktonic cells comparing to biofilm, was glycine-betaine. This compound is the most efficient osmoprotectant compound of *S. aureus*. It also allows this bacteria to grow in the high-salt niches, such as human skin (Graham *et al.*, 1992). Presently, we find no satisfactory explanation for the observed accumulation of glycine-betaine in the planktonic cells, but not in biofilm of *S. aureus*. It may be presumed only, that biofilm cells are better protected than planktonic cells from environmental stress because of extracellular matrix layers. Therefore, more stress-exposed planktonic cells have to use such countermeasures, as glycine-betaine accumulation. Since the observed trend is strong and statistically significant (Fig. 3), further experiments need to be performed to understand this phenomenon.

In the presented work, we showed possibility of discriminating *S. aureus* biofilm from *S. aureus* planktonic form by means of NMR technique. The utility of this method was supported by comparison with SEM microscopy and quantitative culturing. Moreover, our findings, being of preliminary value, if developed, may be helpful in future clinical applications. A limitation of this particular work is that only one *S. aureus* strain was investigated.

The biofilm formation is a complex process depending on plethora of factors. Presently, we are unable to define its specific time-points in *in vivo* clinical setting without using sophisticated, cutting-edge methods. NMR spectroscopy could be considered as one of them and it might find an application in microbial diagnostics in the future.

In conclusion, there are strong differences in metabolite patterns between *S. aureus* biofilm and planktonic cells as indicated by NMR analysis. In this study, a single marker metabolite has not been found as present in one form of bacterial organization, and as completely absent in another one. However, statistically significant differences in specific metabolite concentrations were presented. If to treat these differences in the total manner, pat-

tern obtained may serve as a collective biomarker of the *S. aureus* biofilm presence.

Acknowledgements

Adam F. Junka is a recipient of PBMN-12 grant from Polish Ministry of Science and Higher Education.

Stanislaw Deja is a recipient of a Ph.D. scholarship under project funded by the European Social Fund.

REFERENCES

Bertini I, Cacciatore S, Jensen B, Schou J, Johansen J, Kruhoffer M, Luchinat C, Nielsen D, Turano P (2012) Metabolomic NMR Fingerprinting to Identify and Predict Survival of Patients with Metastatic Colorectal Cancer. *Cancer Res* **72**: 356–364.

Bjarnsholt T, Kirketerp-Møller K, Jensen PØ, Madsen KG, Phipps R, Krogfelt K, Høiby N, Givskov M (2008) Why chronic wounds will not heal: a novel hypothesis. *Wound Rep Reg* **16**: 2–10.

Bjarnsholt T (2011) *Biofilm Infections*. Springer Science, ISBN978-1-4419-6083-2.

Bothwell J, Griffin J (2010) An introduction to biological nuclear magnetic resonance spectroscopy. *Biol Rev Camb Philos Soc* **86**: 493–510.

Declerck P (2010) Biofilms: the environmental playground of Legionella. *Env Microb* **12**: 557–566.

Fiehn O (2002) Metabolomics — the link between genotypes and phenotypes. *Plant Mol Biol* **48**: 155–171.

Gupta A, Dwivedi M, Mahdi A, Khetrapal L, Bhandari M (2012) Broad identification of bacterial type in urinary tract infection using (1)h NMR spectroscopy. *J Proteome Res* **11**: 1844–1854.

Gaupp R, Schlag S, Liebeke M Lak M, Gotz F (2010) Advantage of Upregulation of Succinate Dehydrogenase in Staphylococcus aureus Biofilms. *J Bacteriol* **192**: 2385–2394.

Graham J, Wilkinson B (1992) *Staphylococcus aureus* osmoregulation: roles for choline, glycine betaine, proline, and taurine. *J Bacteriol* **174**: 2711–2716.

Gross M, Cramton S, Gotz F, Peschel A (2001) Key role of teichoic acid net charge in *Staphylococcus aureus* colonization of artificial surfaces. *Infect Immun* **69**: 3423–3426.

Hochbaum A, Kolodkin-Gal I, Foulston L, Kolter R, Aizenberg J, Losick R (2011) Inhibitory effects of D-amino acids on *Staphylococcus aureus* biofilm development. *J Bacteriol* **193**: 5616–5623.

Jawien A *et al.* (2012) Guidelines for local and systemic treatment of infected chronic wounds. *Leczenie Ran* 9: 77–91. (in Polish and English).

Li X, Chen H, Jia W, Xie G (2013) A metabolomics-based strategy for the quality control of traditional Chinese medicine: shengmai infection as a case study. *Evid Based Complemnet alternat Med* doi: 10.1155/2013/836179.

Mahmoud Gad, Abdel Aziz, Ibrahem A (2012) *In-vitro* adhesion of *Staphylococcus* spp. to certain orthopaedic biomaterials and expression of adhesion genes. *J App Pharm Scien* **6**: 145–149.

Montato L, Speziale P, Campoccia D (2011) Scenery of *Staphylococcus* implant infections. *Future Microbiol* **6**: 1329–1349.

Nicholson J, Lindon J, Holmes E (1999) "Metabonomics" understanding the metabolic responses of living systems to pathophysiological stimuli via multivariate statistical analysis of biological NMR spectroscopic data. *Xenobiotica* **29**: 1181–1189.

Pohl K, Francois P, Stenz L, Schlin F, Geiger T, Herbert S, Goerke CH, Schrenzel J, Wolz Ch (2009) CodY in *Staphylococcus aureus*: a regulatory link between metabolism and virulence gene expression. *Infect Immun* **191**: 2953–2963.

Resh A, Rosenstein, Nerz Ch, Gotz F (2005) Differential gene expression profiling of *Staphylococcus aureus* cultivated under biofilm and planktonic conditions. *Appl Envirol Microbiol* **71**: 2663–2673.

Sadowska B, Wieckowska-Szakiel M, Paszkiewicz M, Rozalska B (2013) The immunomodulatory activity of *Staphylococcus aureus* products derived from biofilm and planktonic cultures. *Act Immunol Ther Exp* **61**: 413-420.

Schievano E, Stocchero M, Morelato E, Facchin C, Mammi S (2012) An-NMR-based metabolomic approach to identify the botanical origin of honey. *Metabolomics* **8**: 679–690.

Schlag S, Nerz Ch, Birkenstock T, Altenberend F, Gotz F (2007) Inhibition of *Staphylococcal* biofilm formation by nitrite. *J Bacterial* **189**: 7911–7919.

Secor P, James G, Fleckman P, Olerud J, McInnerney K, Stewart P (2011) *Staphylococcus aureus* biofilm and planktonic cultures differentially impact gene expression, mapk phosphorylation, and cytokine production in human keratinocytes. *BMC Microbiol* **11**: 143. doi: 10.1186/1471-2180-11-143.

Shunmuganperumal T *et al.* (2010) *Biofilm Eradication and Prevention*; John Wiley & Sons, ISBN 978-0-470-47996-4.

Widegrow A (2008) Persistence of the chronic wound — implicating biofilm. *Wound Heal South Afr* **1**: 05–07.

Wolcott R, Rhoads D. (2008) Study of biofilm — based wound management in subjects with cririal limb ischaemia. *J Wound Care* **17**: 145–155.

Wolcott R, Dowd S, Kennedy J, Jones C (2010) Biofilm — based wound care. *Adv in W Care* **1**: 311–318 .

Zhang B, Powers R (2012) Analysis of bacterial biofilms using NMR-based metabolomics. *Fut Med Chem* **4**: 1273–1306